Amygdala stimulation modulates hippocampal synaptic plasticity

Kazuhito Nakao, Koji Matsuyama, Norio Matsuki, and Yuji Ikegaya*

Laboratory of Chemical Pharmacology, Graduate School of Pharmaceutical Sciences, University of Tokyo, 7-3-1 Hongo, Bunkyo-ku, Tokyo 113-0033, Japan

Communicated by James L. McGaugh, University of California, Irvine, CA, August 19, 2004 (received for review February 5, 2004)

Experience-dependent synaptic plasticity is a fundamental feature of neural networks involved in the encoding of information, and the capability of synapses to express plasticity is itself activity-dependent. Here, we introduce a ''low-frequency burst stimulation'' protocol, which can readily induce both long-term potentiation (LTP) and long-term depression (LTD) at *in vivo* medial perforant path–dentate gyrus synapses. By varying stimulation parameters, we were able to build a stimulus–response map of synaptic plasticity as a LTP–LTD continuum. The response curve displayed a bidirectional shift toward LTP and LTD, depending on the degree and timing of neural activity of the basolateral amygdala. The range of this plastic modulation was also modified by past activity of the basolateral amygdala, suggesting that the amygdala can arrange its ability to regulate the dentate plastic responses. The effects of the BLA activation were replicated by stimulation of the lateral perforant path and, hence, BLA stimulation may recruit the lateral entorhinal cortex. These results represent a high-order dimension of heterosynaptic modulations of hippocampal synaptic plasticity.

BCM theory | metaplasticity | long-term potentiation | long-term depression | dentate gyrus

The amygdala plays an important role in emotional arousal and has emerged as a key modulator of memory storage in other brain regions (1, 2). Behavioral studies have indicated that microinjections of diverse pharmacological agents such as glucocorticoid-receptor agonists, β-adrenergic agents, amphetamine, and local anesthetics into the basolateral amygdala (BLA) enhance or impair hippocampus-dependent memory (3–7).

In support of these studies, we and other groups have reported that BLA activation/inactivation or delivery of glutamatergic and β-adrenergic agents into the BLA can modulate long-term potentiation (LTP) at the medial perforant path (MPP)–dentate gyrus (DG) synapses in the hippocampal formation (8–13). Prior stimulation of the BLA is also capable of gating subsequent induction of LTP in the DG (14, 15). The BLA modulation of hippocampal LTP is, therefore, a compelling candidate mechanism underlying the amygdalar control of the hippocampal memory system.

In this respect, however, several issues remain to be resolved. For example, it is uncertain which brain region relays BLA inputs to the DG, which dentate substratum ultimately receives the BLA input, whether the BLA also modulates hippocampal long-term depression (LTD), or how various patterns of BLA activity alter its ability to modulate DG plasticity. In particular, the last two questions have been difficult to address because there is no simple experimental system that can reliably induce homosynaptic LTD *in vivo*; note that, unlike the case of slice preparations, *in vivo* LTD is usually inducible only when the synapses are electrically or pharmacologically primed before a LTD-inducing stimulus (16–19).

In the present work, we describe an *in vivo* protocol of low-frequency burst stimulation (LFBS), which consists of repetitive burst trains, as shown in Fig. 2*A* (20, 21). By changing the number of stimuli in each burst train, we find that LFBS, when delivered to the MPP, can produce varying levels of synaptic plasticity, i.e., a continuum from LTP to LTD, without any priming stimulation (Fig. 2*D*, open circles). This LTP–LTD transition is consistent with the proposal of the Bienenstock–Cooper–Monro (BCM) theory (22), which predicts that the direction and degree of synaptic plasticity will change depending on the pattern of synaptic activation. It has been postulated that the BCM modification threshold is not a constant function but rather is regulated by prior or concurrent neuronal activity. This form of higher-order plasticity may be crucial to secure a broad range of LTP and LTD responses and, at least conceptually, can account for adaptive responses shown by neurons whose activity is manipulated, e.g., visual deprivation (19, 23, 24). We find that such a high-order modulation of MPP–DG synaptic efficacy is indeed brought about by the patterned activity of BLA neurons. Interestingly, this modulation is itself modifiable by the BLA–DG synaptic strength.

Materials and Methods

Field Potential Recordings. Postnatal 9- to 20-week-old (290–390 g) male Wistar/ST rats (SLC, Shizuoka, Japan) were anesthetized with 1 g/kg urethane and 25 mg/kg α-chloralose (i.p.) and fixed in a stereotaxic head holder, according to National Institutes of Health guidelines for laboratory animal care and safety. Unless otherwise specified, two bipolar stimulating electrodes (thin stainless-steel needles coated with epoxy resin except for the 60-μm tip) were placed on the MPP (8.1 mm posterior and 4.4 mm lateral to bregma) and the lateral perforant path (LPP) (8.1 mm posterior and 5.0 mm lateral to bregma) or the BLA (2.8 mm posterior and 5.2 mm lateral to bregma, and 7.6 mm ventral to dura), and a tungsten recording electrode (Frederick Haer, Bowdoinham, ME) was inserted into the dentate molecular layer (3.5 mm posterior and 2.0 mm lateral to bregma) to record field excitatory postsynaptic potentials (fEPSP). Single-pulse test stimuli (80-μs duration) were applied to the MPP at an interval of 30 sec. The stimulus intensity was adjusted to produce a fEPSP with a slope that was $\approx$50% of maximum. To induce associative LTP or LTD at MPP–DG synapses, LFBS that consisted of 600 bursts at 1 Hz was delivered to both the MPP and BLA or LPP. Each burst consisted of 1, 4, 8, 12, 16, 64, or 128 pulses at 250 Hz (Fig. 2*A*). In a series of experiments shown in Fig. 6, theta-burst stimulation (TBS), consisting of five bursts at 5 Hz and 20 pulses at 200 Hz, was applied four times every 30 sec to induce LTP at BLA–DG synapses. The location of electrode was verified with characteristic waveforms evoked by MPP and BLA stimulation (Fig. 1*B*) and post hoc histological observations as described in our previous papers (8, 25). We report the mean $\pm$ SE in all measurements.

Abbreviations: BCM, Bienenstock–Cooper–Monro; BLA, basolateral amygdala; CSD, current source density; DG, dentate gyrus; fEPSP, field excitatory postsynaptic potential; LFBS, low-frequency burst stimulation; LTP, long-term potentiation; LTD, long-term depression; MPP, medial perforant path; LPP, lateral perforant path; TBS, theta-burst stimulation.

*To whom correspondence should be addressed. E-mail: ikegaya@tk.air.jp.

www.pnas.org/cgi/doi/10.1073/pnas.0405709101

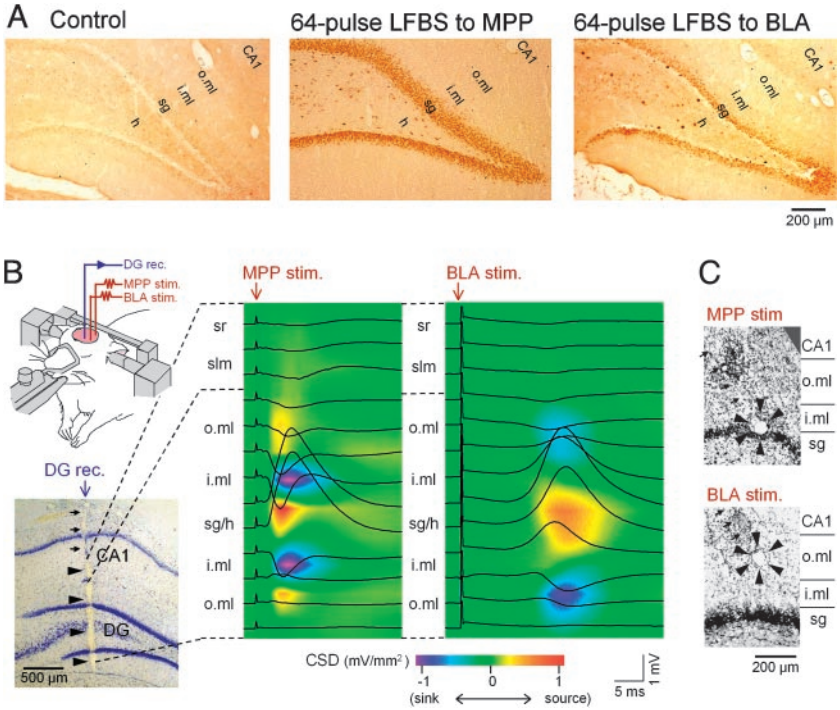

Fig. 1. The BLA excites DG granule cells *in vivo*. (*A*) c-Fos-like immunoreactivity in the DG 120 min after application of a 64-pulse LFBS to MPP (*Center*, $n = 3$) or BLA (*Right*, $n = 3$). The control (*Left*, $n = 5$) received sham implantation of a BLA-stimulating electrode, but no LFBS was delivered. Note the selective induction of c-fos immunoreactivity in granule cells and some hilar cells. (*B*) Laminar profiles of field potentials and their relative CSD recorded in the septal pole of the DG and a part of CA1 after single-pulse stimulation of MPP or BLA. The relative CSD sinks, indicated by ''colder'' colors, were detected in the inner and outer molecular layer after stimulation of MPP and BLA, respectively. The experiments were repeated in four rats, producing similar results. The Nissl image (*Lower Left*) indicates the track of the recording electrode that was marked by making electric lesions at each point of recording. The neighboring lesioned areas were connected, making the long vertical hole. sr, stratum radiatum; slm, stratum lacunosum-moleculare; o.ml, outer molecular layer; i.ml, inner molecular layer; sg, stratum granulosum; and h, hilus. (*C*) Confirmation of the recording site at which MPP- and BLA-evoked CSD sinks reached the maximum. An electric lesion was applied at the site where the largest sink emerged. The arrows and arrowheads in the Nissl images (*B* and *C*) indicate the electrode tracks and lesioned areas, respectively.

Immunohistochemistry for c-Fos. After insertion of a stimulating electrode into the BLA, LFBS with 64-pulse bursts was applied to examine the influence of MPP or BLA activation on c-Fos expression levels in the DG. Two hours after LFBS, rats were transcardially perfused with isotonic PBS, followed by ice-cold 4% paraformaldehyde in 0.1 M phosphate buffer. The brains were removed from the skull. After 2 h of postfixation in 4% paraformaldehyde, they were cropped into an appropriately sized block and coronally cut into 20-μm-thick sections. After being mounted on gelatin-coated glass slides, the sections were incubated in 0.1% Triton X-100 for 15 min, treated with 0.3% H_2O_2 for 20 min, and blocked in 2.5% normal goat serum for 60 min. They were treated with a primary anti-c-Fos antibody (1:3,000; Santa Cruz Biotechnology) at 4°C for 12 h and then with biotinylated anti-rabbit IgG for 1 h. The preparations were processed by using the Elite ABC method (Vector Laboratories) and coverslipped with malinol.

Current Source Density Analysis. The recording electrode was raised, in 100-μm increments, across the DG and CA1. At each interval, at least 3 min of data were recorded, and four responses were evoked every 10 sec and averaged. The uniform cytoarchitecture of the DG, including segregation of afferents into laminae and stereotypic dendritic orientation, allows the current source density (CSD) computation to simplify to one spatial dimension (26). Specifically, the extracellular membrane current density is estimated as the second spatial derivative of the field potential and is computed by using a 3–5 spatial-point formula.

Results

BLA Excites DG Granule Cells. Our initial set of experiments was designed to elucidate the amygdalar influence on hippocampal excitability. As part of this effort, we used c-Fos-like immunoreactivity, a marker of neuronal activation (27). In anesthetized rats, we delivered LFBS, consisting of 64-pulse burst trains, to the BLA (see Fig. 2*A*). After 120 min, we compared c-Fos-like immunoreactivity with that of control animals. Although there was no apparent immunoreactivity in the hippocampal formation under basal conditions, the signal became evident in the granule cell layer and some hilar cells after BLA stimulation (Fig. 1*A*). The induction of c-Fos-like immunoreactivity occurred only in the DG ipsilateral to the stimulated BLA (data not shown). As a control experiment, the same condition of LFBS was delivered to the MPP. c-Fos expression was induced in the whole-granule cell layer, including the subgranular zone. These data suggest that DG neurons are massively activated by LFBS of the BLA as well as MPP.

We next sought to characterize the projections from the BLA to the temporal pole of the DG by comparing field potentials evoked by single-pulse stimulation of the MPP and BLA. Stimulation of the MPP elicited an early potential with a peak amplitude delay of 6.68 ± 0.14 msec (Fig. 1*B*, $n = 31$). The relative CSD profiles showed a large sink associated with the component of field-negative potentials; the largest sink was observed in the inner/middle part of the DG molecular layer. BLA stimulation produced the largest CSD sink in the outer molecular layer, with a latency of 18.29 ± 0.56 msec (Fig. 1*B*, $n = 31$). To confirm the position of the recording electrode, we

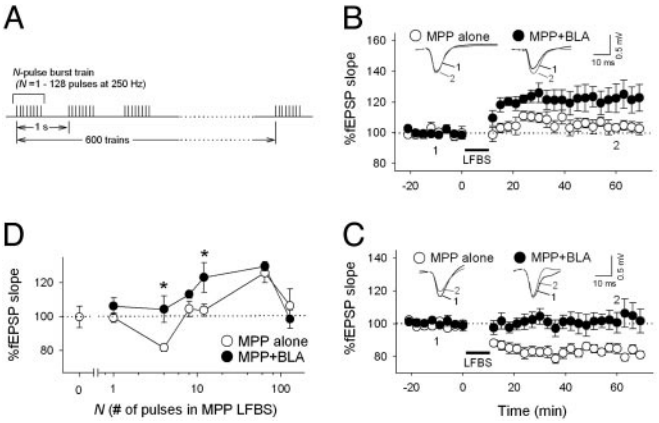

Fig. 2. Strong BLA activation induces an upward shift of the BCM-like threshold for MPP–DG synaptic modification. (*A*) Protocols of LFBS used to induce LTP or LTD. LFBS consists of 600-burst trains spaced at 1 sec. Each burst consists of 1–64 pulses at 250 Hz. LFBS was simultaneously applied to the MPP and BLA unless otherwise specified. LFBS containing 12-pulse (*B*) or 4-pulse (*C*) bursts was delivered to the MPP without (MPP alone) or together with 64-pulse LFBS to the BLA (MPP+BLA). Time course of fEPSP slopes is expressed as percentage of baseline. Representative recordings at −10 (1) and 60 (2) min are shown in *Insets*. (*D*) Summary data for varying pulses of LFBS to the MPP (0, 1, 4, 8, 12, 64, and 128 pulses). Zero pulse means that LFBS was applied to the BLA alone. The ordinate indicates fEPSP slopes averaged from 50 to 60 min. *, $P < 0.05$ vs. MPP alone; Student's *t* test. Data are means ± SE of five to nine rats.

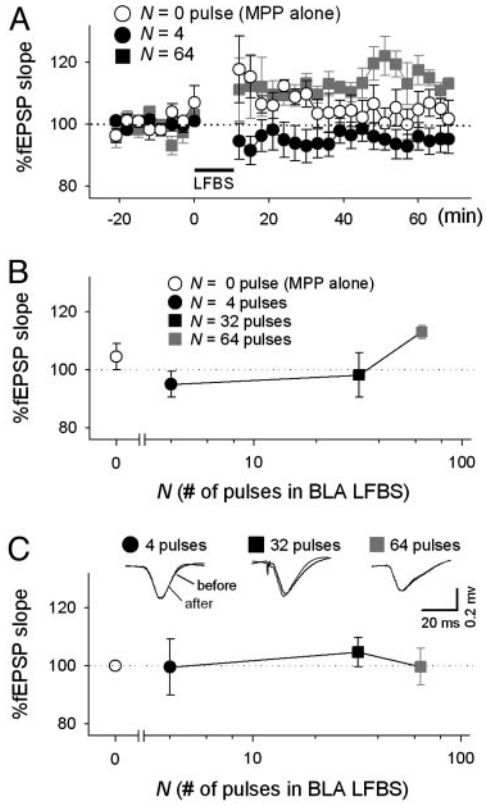

Fig. 3. Temporal patterns of BLA activation determine bidirectional modulations of MPP–DG synaptic plasticity. (*A*) LFBS of 8-pulse bursts was applied to the MPP, combined with LFBS of 0, 4, and 64 pulses to the BLA. (*B*) Summary data for varying pulses of BLA LFBS (0, 4, 32, and 64 pulses). Zero pulse (○) means MPP LFBS applied alone (without BLA LFBS). BLA LFBS of 64 pulses augmented MPP–DG LTP, whereas 4-pulse BLA LFBS suppressed LTP and induced LTD. (*C*) The effect of BLA LFBS alone on baseline MPP–DG synaptic responses. Various pulses of LFBS (0, 4, 8, 32, and 64 pulses) were applied without MPP LFBS. Representative recordings at −10 (before) and 60 (after) min are shown in *Insets*. BLA LFBS alone had no effect on basal transmission at MPP–DG synapses. Data are means ± SE of 4–10 rats.

performed an electric lesion to mark the site where the maximal CSD sink was recorded. The lesioned sites were found in the inner and outer molecular layer for MPP and BLA stimulation, respectively (Fig. 1*C*). Therefore, the MPP and BLA projections terminate on distinct dendritic regions of DG granule cells; that is, the BLA innervates a more distal portion of dendrites than the MPP. The long latency of BLA-evoked responses suggests that the projection may be polysynaptic. Considering that the CSD sink reached the maximum in the outer molecular layer, BLA stimulation seems to activate the dentate gyrus through the LPP.

BLA Bidirectionally Regulates Bidirectional Synaptic Plasticity at MPP–DG Synapses. Our previous study has indicated that simultaneous tetanization of the MPP and BLA facilitates the induction of LTP at MPP–DG synapses, i.e., associative LTP (8, 28). We confirmed whether the same phenomenon was induced by the LFBS protocol. During application of mild LFBS (12-pulse bursts) to the MPP, the BLA was strongly activated by LFBS of 64-pulse bursts (Fig. 2*B*). Immediately after LFBS, MPP–DG synaptic transmission was enhanced, and this potentiation was maintained during >60 min of our observation period (Fig. 2*B*, closed circles). On average, MPP-evoked fEPSP slopes 50–60 min after LFBS were increased by 23.0 ± 8.8% from the preLFBS level, indicative of LTP ($n = 5, P < 0.01$, paired *t* test), although MPP LFBS alone induced no apparent change (3.7 ± 3.5%, $n = 5, P > 0.1$) (Fig. 2*B*, open circles). Thus, BLA LFBS augments MPP LFBS-induced LTP at MPP–DG synapses.

To determine whether BLA activity also affects the induction of LTD at MPP–DG synapses, we applied weaker LFBS to the MPP. LFBS consisting of four-pulse bursts was found to induce LTD at MPP synapses; the fEPSP slopes were decreased by 18.4 ± 2.3% from baseline (Fig. 2*C*, $n = 9$, $P < 0.01$). Interestingly, when coupled with 64-pulse LFBS of BLA, the MPP LFBS did not induce LTD, the change in fEPSPs being only 4.3 ± 7.9% (Fig. 2*C*, $n = 7$). Thus, BLA activation abolished LTD at MPP synapses.

Likewise, the impact of 64-pulse BLA LFBS was examined for various conditions of MPP LFBS, i.e., 1, 4, 8, 12, 64, and 128 pulses of burst. Data are summarized in Fig. 2*D*. In the absence of BLA stimulation, MPP synapses displayed bidirectional modulations of plasticity, depending on the number of stimuli involved in individual bursts of MPP LFBS. As a result, the stimulus–response function showed a BCM-like sigmoidal curve (Fig. 2*D*, open circles). When LFBS were simultaneously delivered to the BLA, this stimulus–response curve shifted upward (Fig. 2*D*, closed circles). BLA activation, therefore, causes MPP synapses to favor LTP. Because BLA LFBS alone had no apparent effect on basal MPP–DG synaptic responses (Fig. 3*C*), the BLA modulations represent a nonlinear associative interaction between MPP–DG and BLA–DG synapses.

In the next set of experiments, we alternatively measured the effects of a varying number of BLA pulses on a constant number of MPP pulses. The BLA was stimulated by 4-, 32-, or 64-pulse LFBSs during 8-pulse MPP LFBS. As shown above, 64-pulse BLA LFBS facilitated the induction of LTP triggered by 8-pulse MPP LFBS (Fig. 3*A*). Surprisingly, 4-pulse BLA LFBS rather suppressed the LTP induction, even leading to LTD (Fig. 3*A*). Depending on its intensity, BLA LFBS seems to be capable of enhancing or blocking LTP at MPP–DG synapses (Fig. 3*B*).

To evaluate these results in more details, we delivered 4-pulse LFBS to the BLA during MPP LFBS with varying pulses (1, 2, 8, 16, and 64 pulses). Four-pulse BLA LFBS attenuated 16-pulse

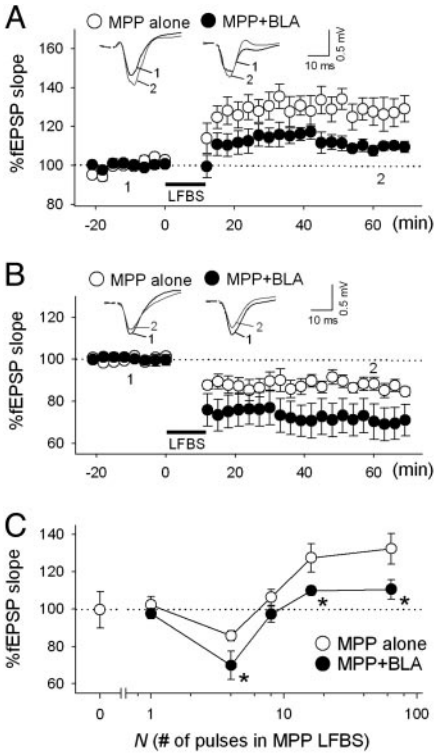

Fig. 4. Weak BLA activation induces a downward shift of the BCM-like curve of MPP–DG synaptic plasticity. (*A* and *B*) LFBS containing 4-pulse bursts (*B*) or 16-pulse bursts (*A*) was delivered to the MPP without (MPP alone) or together with 4-pulse LFBS of the BLA (MPP+BLA). Representative recordings at time −10 (1) and 60 (2) min are shown in *Insets*. (*C*) Summary data for varying pulses of MPP LFBS (0, 1, 4, 8, 16, and 64 pulses). *, $P < 0.05$ vs. MPP alone; Student's *t* test. Data are means ± SEM of five to eight rats.

MPP–LFBS-induced LTP (Fig. 4*A*) and enhanced 4-pulse MPP–LFBS-induced LTD (Fig. 4*B*). In contrast to Fig. 2*C*, the summary data now reveal that the BCM-like curve shifted downward (Fig. 4*C*). Thus, weak BLA activation causes MPP–DG synapses to prefer LTD. Taken together, we conclude that the BLA can bidirectionally control MPP plasticity.

Synaptic responses monitored during LFBS are shown in Fig. 7, which is published as supporting information on the PNAS web site. Prolonged activation of the BLA tended to attenuate late responses evoked by a long MPP LFBS.

BLA Modulations Require a Specific Time Window for BLA Activation. We examined the effect of the relative timings of application of BLA and MPP LFBS on MPP–DG plasticity. Conditioning paradigms of stimulation used here are shown in Fig. 5*A*; 12-pulse MPP LFBS was started 15 msec before ($\Delta t = -15$ ms) or 15 msec after ($\Delta t = 15$ ms) the onset of 64-pulse BLA LFBS, and their effects were compared with that of MPP LFBS applied concurrently with BLA LFBS ($\Delta t = 0$ ms). We found that the efficiency of BLA LFBS to enhance MPP–DG LTP was maximal at $\Delta t = 0$ ms (Fig. 5 *B* and *C*).

Our CSD analysis of BLA-evoked DG responses suggests that BLA inputs terminate in the outer molecular layer of the DG in a polysynaptic fashion. Because the lateral entorhinal cortex sends the LPP axons to the outer molecular layer (29) and because this cortical area receives a monosynaptic input from the BLA (30), it is plausible that the LPP relays BLA inputs to the DG. If this hypothesis is true, LFBS of the LPP is expected to modulate MPP plasticity, like BLA LFBS. We examined the LPP with the same differential timing protocol (Fig. 5*A*). As expected, LPP LFBS enhanced MPP LTP, but, interestingly, the effect was largest at $\Delta t = 15$ ms (Fig. 5*C*), which plausibly corresponds with the delay of one synaptic step from the BLA to the lateral entorhinal cortex. The sensitivity of MPP and LPP interaction to differential timings may be consistent with previous papers showing that timings of activity between ipsilateral and contralateral perforant path afferents affect their plastic responses (31, 32).

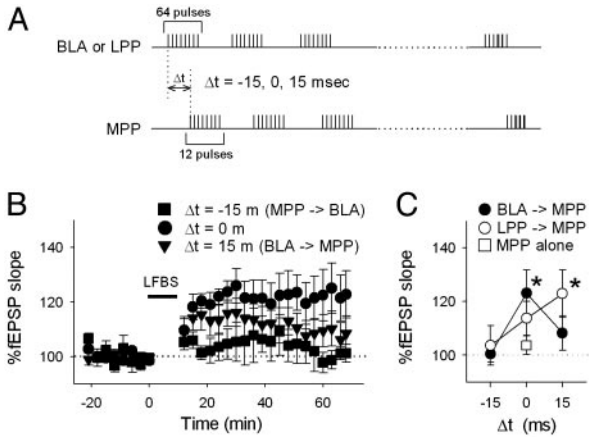

Fig. 5. BLA modulations of MPP plasticity depend on relative activation timings of the BLA and MPP. (*A*) Stimulation protocols. Twelve-pulse MPP LFBS started −15, 0, or 15 msec after the onset of 64-pulse LFBS of BLA or LPP. (*B*) LFBS was delivered to MPP 15 msec before ($\Delta t = -15$ ms), concurrently with ($\Delta t = 0$ ms), or 15 msec after BLA LFBS ($\Delta t = 15$ ms). (*C*) Summary data for relative timing of LFBS of the BLA and LPP. *, $P < 0.05$ vs. MPP alone; Student's *t* test. Data are means ± SEM of four to six rats.

BLA–DG Synaptic Strength Determines Its Ability of MPP Synaptic Modulation. BLA–DG postsynaptic potentials displayed LTP and LTD in response to TBS and four-pulse LFBS applied to the BLA, respectively (Fig. 6*A*). This finding indicates that, like MPP–DG synapses, the BLA–DG transmission is also subject to bidirectional plastic modifications. We thus hypothesized that the potency of the BLA to modulate MPP–DG synaptic plasticity is itself changed by BLA–DG plasticity. To address this possibility, we delivered either TBS or LFBS to the BLA (priming stimulation) to change the strength of BLA–DG synapses. Five minutes after this priming stimulation, the MPP and BLA were jointly stimulated with eight- and four-pulse LFBS, respectively ($\Delta t = 0$ msec). Depending on the types of BLA priming, the joint stimulation of MPP and BLA produced distinct degrees of synaptic modifications: When TBS was applied to BLA, subsequent LFBS of MPP and BLA induced LTP (Fig. 6*B Upper*), whereas it induced LTD when four-pulse LFBS was used as a BLA priming (Fig. 6*B Lower*). Importantly, the slopes of BLA-evoked fEPSPs after priming and before MPP–DG stimulation correlated with the capacity of the BLA to modulate MPP–DG plasticity (Fig. 6*C*), indicating that the synaptic strength of the BLA–DG pathway determines its ability to modulate MPP–DG plasticity. The history of BLA activity (BLA priming status) is therefore manifest in the MPP–DG synaptic modulation threshold.

Akirav and Richter-Levin (33) showed that prior BLA activation can gate the induction of LTP at MPP–DG synapses. In our experimental system, however, we found no evidence for such a priming effect of BLA activation, at least for our LFBS protocol: Prior stimulation of the BLA did not affect LTP induced by sequence LFBS to MPP alone (Fig. 6*D*), in agreement with a previous study (8). This apparent discrepancy may be due to the interval between BLA priming and LTP induction. In most experiments by Akirav and Richter-Levin, they applied

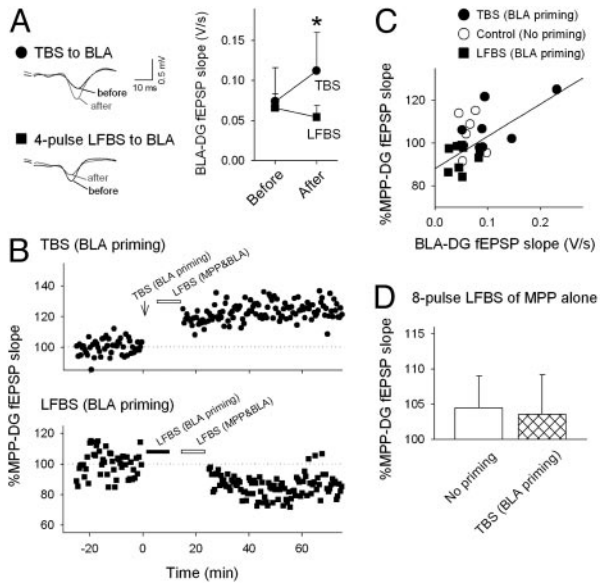

Fig. 6. History-dependent BLA control of MPP–DG plasticity. (*A*) Plasticity displayed by BLA–DG synapses. The ordinate (*Right*) indicates the slopes of BLA-evoked fEPSPs in the DG. The traces (*Left*) represent BLA-evoked DG responses 5 min before and 5 min after application of either TBS or four-pulse LFBS to the BLA. *, $P < 0.05$ vs. before; paired *t* test. Data are means ± SE of each five to eight rats. (*B*) Representative time courses of MPP-evoked fEPSPs after coapplication of eight-pulse MPP LFBS and four-pulse BLA-LFBS 5 min after priming stimulation of either TBS (*Upper*) or LFBS (*Lower*) to the BLA. MPP plasticity was induced 5 min after the BLA priming. (*C*) Positive correlations between BLA–DG synaptic strength and the degree of the BLA modulation of MPP synaptic plasticity. The ordinate indicates fEPSP slopes from 50 to 60 min after application of MPP–BLA LFBS, which was applied 5 min after BLA priming (TBS or LFBS). The abscissa indicates BLA–DG fEPSP slopes immediately before the induction of MPP plasticity. Each symbol represents one animal. Solid lines are the best linear fit to the data ($r = 0.547$, df = 22; $P = 0.006$). (*D*) Lack of the effect of BLA priming on homosynaptic modifications induced by LFBS of the MPP alone. TBS was applied to the BLA 5 min before eight-pulse LFBS of the MPP. Data are the average of fEPSP slopes from 50 to 60 min after MPP LFBS (means ± SE of five rats).

high-frequency stimulation to the MPP only 30 sec after the priming (33).

Discussion

Electrophysiological studies have recently implicated the amygdala as a modulator of hippocampal LTP, but the specific nature of this regulation remains to be elucidated. By developing a stimulation protocol that can reliably induce bidirectional synaptic plasticity, LFBS, this work has succeeded in delineating transitions between LTP and LTD as a function of the stimulus intensity *in vivo*, i.e., a map relevant to BCM theory. The LFBS protocol allowed us to investigate the heterosynaptic modulation of bidirectionally hippocampal plasticity by synaptic inputs from the amygdala. We have shown that BLA inputs in the DG are independent of MPP afferents and that strong BLA activation decreases the LTP/LTD-crossover threshold to favor LTP, whereas weak BLA activation increases it. Moreover, this modulation threshold varied depending on the strength of BLA–DG synaptic connections.

Neural Projections from BLA to DG. After stimulation of the BLA, c-Fos expression was induced in virtually all DG granule cells, suggesting that the BLA influence on the DG is widespread. Indeed, BLA stimulation elicited a robust CSD sink in the outer molecular layer in both the suprapyramidal and infrapyramidal blades of the DG. BLA is, hence, likely to activate the entire DG by excitatory synapses with a distal part of dendrites of granule cells. Because the MPP terminates on a more proximal part of dendrites, the BLA and MPP inputs presumably synapse on distinct dendritic segments of DG granule cells, and their interactions may be uniquely shaped by dendritic membrane properties. Consistent with this idea is our previous study showing a temporal interaction of MPP-evoked action potentials and BLA-elicited EPSPs in the DG (25).

The anatomical pathway of the BLA–DG connection cannot be determined by our data alone. However, considering a BLA-evoked CSD sink in the outer molecular layer with a long latency (Fig. 1 and ref. 33), we suggest that BLA inputs may be relayed by the lateral entorhinal cortex, which receives a direct projection from the BLA (30) and sends its LPP axons to the DG molecular layer (31). Indeed, we found that LPP and BLA are both capable of enhancing MPP–DG LTP. In this respect, BLA is not necessarily the unique region that can modulate MPP plasticity. It is rather feasible that activation of other excitatory inputs to the lateral entorhinal cortex would have the same capability. Alternatively, the septohippocampal pathway could provide the relay between the BLA and DG, because reinforcement of early DG LTP into late LTP by the BLA is blocked by surgical transaction of the fimbria–fornix pathway (13).

Metamodulations of Hippocampal Metaplasticity by BLA. If excitatory inputs from independent afferents coincide on the same dendrite, they yield larger depolarization in the postsynaptic cell, leading to the induction of LTP. This paradigm, termed "associativity," is a common feature of LTP induction (34). In this sense, the fact that the BLA facilitates MPP–DG LTP is not surprising because BLA readily evokes EPSPs in the DG. However, in the case of four-pulse LFBS, BLA activation attenuated LTP and even augmented LTD. We therefore do not believe that the simple summation of EPSPs provides full explanations for the mechanisms by which the BLA modulates MPP plasticity. Discharges of BLA neurons are known to generate synchronized activity (termed sharp potentials) in the entorhinal cortex, which in turn induces subthreshold oscillations in the DG (35). It is hence feasible that BLA LFBS elicits phasic fluctuations of membrane potential in DG granule cells and that their phase correlations with MPP LFBS pulses determine the direction of synaptic modification, similar to spike timing-dependent plasticity (36). This notion is compatible with the existence of a narrow time window during which BLA LFBS may modulate MPP plasticity (Fig. 5). It is still possible that the BLA modulation is not mediated by BLA-evoked EPSPs; for example, peripheral norepinephrine and corticosterone may contribute (16). We consider, however, that these hormonal mediators are unlikely to participate, because the amplitude of the BLA modulation correlated with the BLA–DG synaptic strength (Fig. 6*C*).

The BCM theory proposes that the stimulus–response curve will shift left or right along the horizontal axis as a function of postsynaptic activity (22). In our results, however, the curve seems more likely to shift up or down along the vertical axis. Such a pseudovertical shift of the BCM curve has been predicted in a theoretical model (37). Our empirical data may thus provide evidence for the existence of this mode of synaptic modification. Importantly, the BLA–DG synaptic strength has a crucial influence on the potency of BLA modulation. Therefore, three different factors are now described that control MPP–DG synaptic efficacy. First, the level of MPP–DG synaptic activation defines the direction and degree of homosynaptic plasticity along a BCM-like sinusoidal curve, representing the classical concept of synaptic modification (see Fig. 8*A*, which is published as supporting information on the PNAS web site). Second, the BCM-like curve shifts depending on the BLA–DG heterosynaptic activity, indicative of a bidirectional associative synaptic

plasticity. If BLA–DG synaptic activity is low during MPP–DG activation, the curve moves downward to favor LTD, but if the activity exceeds a certain threshold, the curve moves upward to favor LTP (Fig. 8*B*). Third, these dynamics of BLA modulation are scaled by the strength (and thus the recent history) of BLA–DG synaptic transmission, i.e., state-dependent associative plasticity. Stronger BLA–DG connections can modulate MPP plasticity more efficiently, whereas weaker connections require higher levels of the BLA activity for obtaining the same extent of the effect (Fig. 8*C*). This model for the high-order dynamics of synaptic modifications lends insight into the external regulatory system of hippocampal physiology.

Because DG neuron activity constitutes the principal input to the hippocampus, this work suggests that neuronal activity of the amygdala can modulate information transfer into the hippocampus. The hippocampal formation is firmly established as being necessary for the formation and retention of declarative memories (38, 39). Therefore, the amygdalar metacontrol of hippocampal plasticity may represent a neural correlate of the amygdalar modulation of hippocampus-dependent memory and thus suggests a mechanism for the well known role of emotional salience in memory (1, 2).

We are grateful to Mr. Neil A. Gray (Columbia University, New York) for his critical review of the manuscript.

1. McGaugh, J. L. (2000) *Science* **287,** 248–251.
2. McGaugh, J. L. (2004) *Annu. Rev. Neurosci.* **27,** 1–28.
3. Roozendaal, B. & McGaugh, J. L. (1997) *Neurobiol. Learn. Mem.* **67,** 176–179.
4. Vazdarjanova, A. & McGaugh, J. L. (1999) *J. Neurosci.* **19,** 6615–6622.
5. Hatfield, T. & McGaugh, J. L. (1999) *Neurobiol. Learn. Mem.* **71,** 232–239.
6. Packard, M. G. & Teather, L. A. (1998) *Neurobiol. Learn. Mem.* **69,** 163–203.
7. Packard, M. G., Cahill, L. & McGaugh, J. L. (1994) *Proc. Natl. Acad. Sci. USA* **91,** 8477–8481.
8. Ikegaya, Y., Saito, H. & Abe, K. (1995) *Neurosci. Res.* **22,** 203–207.
9. Ikegaya, Y., Nakanishi, K., Saito, H. & Abe, K. (1997) *NeuroReport* **8,** 3143–3146.
10. Ikegaya, Y., Saito, H. & Abe, K. (1995) *Brain Res.* **671,** 351–354.
11. Ikegaya, Y., Saito, H. & Abe, K. (1994) *Brain Res.* **656,** 157–164.
12. Frey, S., Bergado-Rosado, J., Seidenbecher, T., Pape, H. C. & Frey, J. U. (2001) *J. Neurosci.* **21,** 3697–3703.
13. Jas, J., Almaguer, W., Frey, J. U. & Bergado, J. (2000) *Brain Res.* **861,** 186–189.
14. Akirav, I. & Richter-Levin, G. (1999) *Neurosci. Lett.* **270,** 83–86.
15. Akirav, I. & Richter-Levin, G. (2002) *J. Neurosci.* **22,** 9912–9921.
16. Holland, L. L. & Wagner, J. J. (1998) *J. Neurosci.* **18,** 887–894.
17. Manahan-Vaughan, D. (1998) *Neuropharmacology* **37,** 1459–1464.
18. Christie, B. R. & Abraham, W. C. (1992) *Neuron* **9,** 79–84.
19. Abraham, W. C., Mason-Parker, S. E., Bear, M. F., Webb, S. & Tate, W. P. (2001) *Proc. Natl. Acad. Sci. USA* **98,** 10924–10929.
20. Nakao, K., Ikegaya, Y., Yamada, M. K., Nishiyama, N. & Matsuki, N. (2002) *Eur. J. Neurosci.* **16,** 970–974.
21. Nakao, K., Ikegaya, Y., Yamada, M. K., Nishiyama, N. & Matsuki, N. (2003) *Synapse* **47,** 163–168.
22. Bienenstock, E. L., Cooper, L. N. & Munro, P. W. (1982) *J. Neurosci.* **2,** 32–48.
23. Abraham, W. C. & Bear, M. F. (1996) *Trends Neurosci.* **19,** 126–130.
24. Abraham, W. C. & Tate, W. P. (1997) *Prog. Neurobiol.* **52,** 303–323.
25. Ikegaya, Y., Saito, H. & Abe, K. (1996) *Brain Res.* **718,** 53–60.
26. Freeman, J. A. & Nicholson, C. (1975) *J. Neurophysiol.* **38,** 369–382.
27. West, A. E., Griffith, E. C. & Greenberg, M. E. (2002) *Nat. Rev. Neurosci.* **3,** 921–931.
28. Ikegaya, Y., Saito, H. & Abe, K. (1996) *Eur. J. Neurosci.* **8,** 1833–1839.
29. Hjorth-Simonsen, A. (1972) *J. Comp. Neurol.* **146,** 219–232.
30. Krettek, J. E. & Price, J. L. (1977) *J. Comp. Neurol.* **172,** 723–752.
31. Levy, W. B. & Steward, O. (1983) *Neuroscience* **8,** 791–797.
32. Levy, W. B., Brassel, S. E. & Moore, S. D. (1983) *Neuroscience* **8,** 799–808.
33. Akirav, I. & Richter-Levin, G. (1999) *J. Neurosci.* **19,** 10530–10535.
34. Bliss, T. V. & Collingridge, G. L. (1993) *Nature* **361,** 31–39.
35. Pare, D., Dong, J. & Gaudreau, H. (1995) *J. Neurosci.* **15,** 2482–2503.
36. Bi, G. & Poo, M. (2001) *Annu. Rev. Neurosci.* **24,** 139–166.
37. Beggs, J. M. (2001) *Neural Comput.* **13,** 87–111.
38. Squire, L. R. & Zola-Morgan, S. (1991) *Science* **253,** 1380–1386.
39. Eichenbaum, H. (1997) *Annu. Rev. Psychol.* **48,** 547–572.

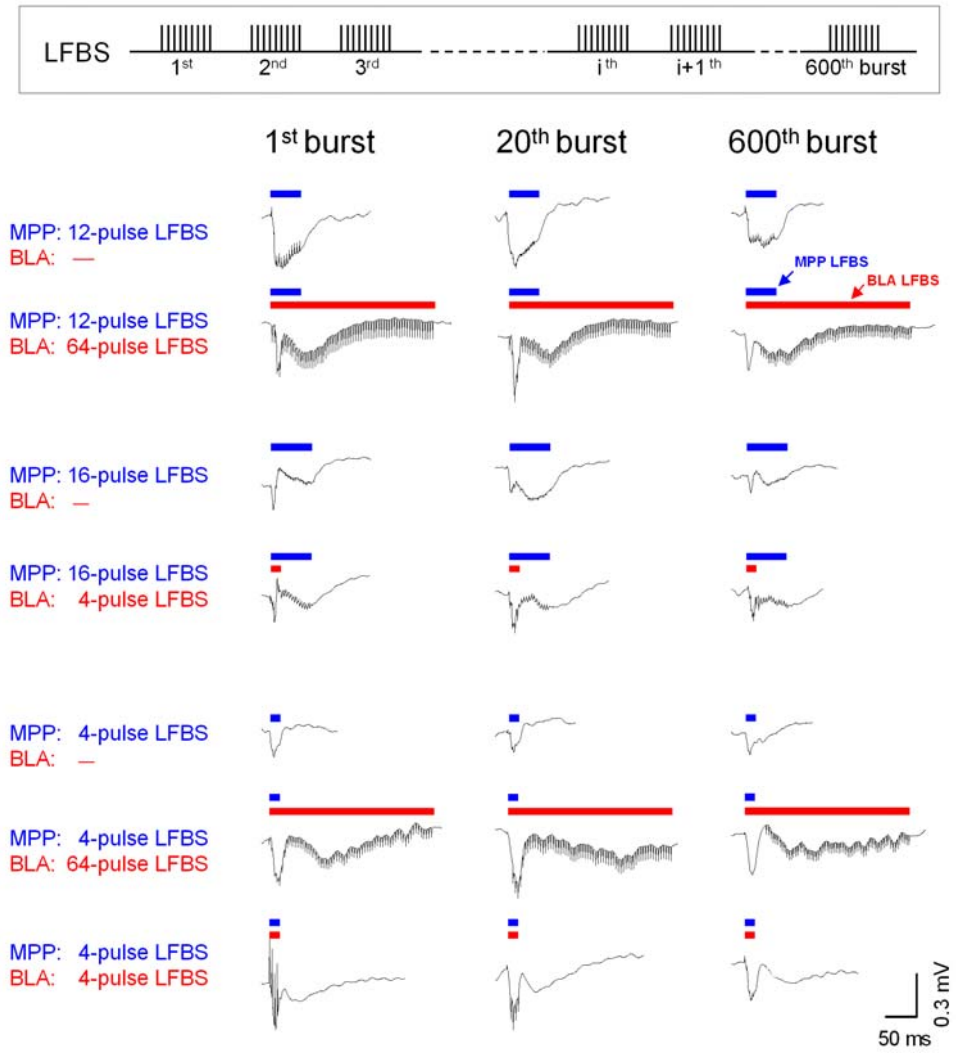

Supporting Fig. 7. Responses during LFBS trains. Traces show field responses to the 1st, 20th, and 600th bursts in LFBS of various conditions of LFBS applied to the MPP and BLA .

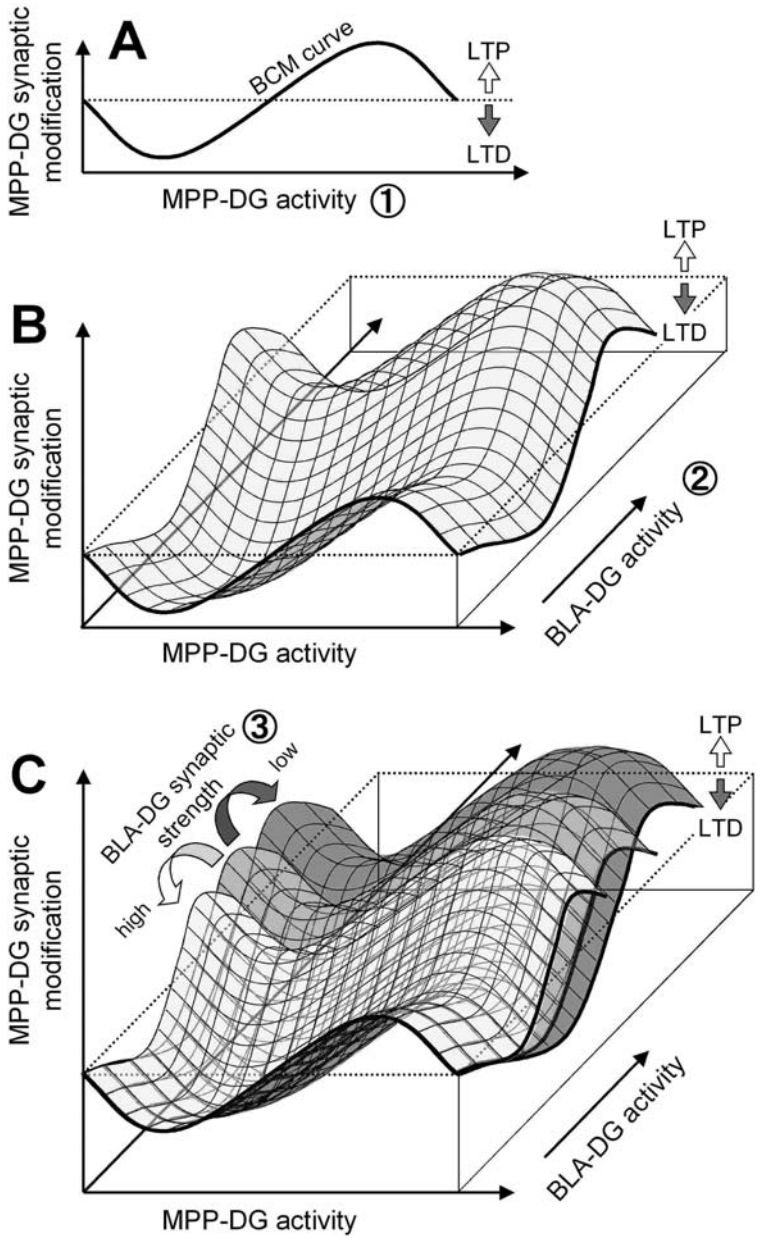

Supporting Fig. 8. 3D representations of the interplay of MPP-DG and BLA-DG synaptic transmission. **A:** First dimension of plastic modulations. The degree of MPP-DG synaptic activation determines the direction of homosynaptic modification, depicting a BCM-like sinusoidal curve. **B:** Second dimension of plastic modulations. The BCM-like curve is subject to BLA-DG heterosynaptic activity-dependent variation, making a pseudo-vertical shift as BLA activity increases. **C:** Third dimension of plastic modulations. The capacity of the BLA to modulate MPP plasticity is itself modulated by synaptic efficacy of BLA-DG transmission, i.e., state-dependent neuromodulation of MPP plasticity.